

Stabilization by deflation for sparse dynamical systems without loss of sparsity

Antonio Cazzani^{a,*}, Peter Ruge^{a,b}

^a*University of Cagliari, DICAAR — Dept. of Civil and Environmental Engineering and Architecture, 2, via Marengo, I-09123 Cagliari, Italy*

^b*Technische Universität Dresden, Institut Statik und Dynamik der Tragwerke, D-01062 Dresden, Germany*

Abstract

Multiple-Input, Multiple-Output models for coupled systems in structural dynamics including unbounded domains, like soil or fluid, are characterized by sparse system-matrices and unstable parts in the whole set of solutions due to spurious modes. Spectral shifting with deflation can stabilize these unstable parts; however the originally sparse system-matrices become fully populated when this procedure is applied.

This paper presents a special consecutive treatment of the deflated system without losing the numerical advantages from sparsity. The procedure starts with an LU -decomposition of the sparse undeflated system and continues with restricting the solution space with respect to deflation using the *same* LU -decomposition. An example from soil-structure interaction shows the benefits of this consecutive treatment.

Keywords: Spurious modes, Deflation, Sparse systems, Stabilization, Unbounded domains

1. Introduction

Dynamic systems play a key-role in engineering and natural sciences. For linear systems the mathematical formulation can be established in the frequency-domain or in the time-domain.

*Corresponding author. Tel: +39-070-6755420; Fax: +39-070-6755418.
Email addresses: antonio.cazzani@unica.it (Antonio Cazzani),
peter.ruge@tu-dresden.de (Peter Ruge)

1 In structural dynamics the equations of motion are of second order in the
 2 time-domain; however by introducing, besides the generalized displacements
 3 \mathbf{u} , the velocities $\mathbf{v} = \dot{\mathbf{u}}$ as additional state variables—after a classical finite
 4 element discretization in the space-domain—a first order differential equation
 5 in the time-domain comes out:

$$\mathbf{A}\dot{\mathbf{z}} - \mathbf{B}\mathbf{z} = \mathbf{f}, \quad \mathbf{z} = \begin{bmatrix} \mathbf{u} \\ \mathbf{v} \end{bmatrix}. \quad (1)$$

6 The homogeneous equation is solved by the exponential $\mathbf{z} = \hat{\mathbf{z}} \exp(\lambda t)$, $\lambda =$
 7 $\alpha + i\beta$ and thus the corresponding linear algebraic equation in the frequency
 8 or spectral domain appears:

$$\lambda \mathbf{A}\hat{\mathbf{z}} - \mathbf{B}\hat{\mathbf{z}} = \mathbf{0}. \quad (2)$$

9 The eigenvalues λ contain the eigenfrequencies β of the system, while the
 10 coefficient α decides upon the stability of the process. Thus, λ is a significant
 11 genetic code of the process.

12 However the linear representation in the spectral domain does not appear
 13 automatically or in every case; there are problems, especially those including
 14 unbounded domains like soil, air, liquid with energy radiation towards in-
 15 finity, which are formulated by means of rational functions which are highly
 16 nonlinear with respect to the eigenvalue λ .

17 Typically, realizations for such problems aim at a state-space formulation
 18 using finitely many samples of impedances; in structural analysis they are
 19 called dynamic stiffnesses. The impedance describes the relation between the
 20 input $f_c = \hat{f}_c \exp(i\Omega t)$ and the output $u_c = \hat{u}_c \exp(i\Omega t)$ at a certain point C
 21 placed, for instance, in the coupling interface between two domains.

22 These samples are taken to establish a rational interpolation like a Padé
 23 one for the impedance K_c :

$$K_c \hat{u}_c = \hat{f}_c, \quad K_c = \frac{P_0 + \lambda P_1 + \lambda^2 P_2 + \cdots + \lambda^{M+1} P_{M+1}}{1 + \lambda q_1 + \lambda^2 q_2 + \cdots + \lambda^M q_M}, \quad \lambda = i\Omega, \quad (3)$$

24 as it is shown in (3), for the sake of simplicity, for a Single-Input, Single-
 25 Output (SISO) problem.

26 In such situations the introduction of additional so-called internal vari-
 27 ables allows a corresponding linear representation in the spectral domain and
 28 thus a first order differential equation in the time-domain.

This can be combined with the classical finite element formulation for the *near field* (a bounded one: e.g. any building, dam, machine, etc.) which is coupled with the unbounded domain, acting as a *far field*. At the very end of this process the representation turns out to become a classical one similar to equation (1).

However it has been realized in relevant studies, especially those dealing with the powerful Scaled Boundary Finite Element Method (SBFEM), that the rational interpolation with the coefficients P_j , Q_j for the unbounded domain is a rather sensitive process and can be contaminated by numerical noise, finally resulting in unstable solutions of the whole coupled problem with positive values α . Indeed, it has been found in papers like [1], [2], [3], [4], [5] that the stability of the dynamic system (2) in the time-domain is not guaranteed *a priori*.

Indeed, these parameters P_j , Q_j are calculated by means of a least-square procedure and only small changes in this procedure can shift eigenvalues from the right side to the left side of the complex plane.

By deflation, these spurious modes can be stabilized but with a significant disadvantage: the block-tridiagonal sparsity of the final matrix \mathbf{B} representing the whole problem, coupling the unbounded and bounded domains (i.e. the *far field* and the *near field*) is lost. How this can be avoided is the main concern of this contribution.

Spurious modes due to numerical noise can happen, too, in system identification; deflation and spectral shifting can be organized there in a similar effective manner.

A different class of linear problems, transient diffusion in unbounded domains, is characterized a priori by only first-order derivatives with respect to time, that is the flux. By means of the SBFEM similar impedances as those defined for structural dynamics can be established, but this time with $\lambda = \sqrt{i\Omega}$.

Thus, the resulting state equation in the frequency-domain, corresponding to (2), contains the frequency Ω in a non-rational manner, since λ is linked to Ω through its square root. Hence:

$$\sqrt{i\Omega}\mathbf{A}\hat{\mathbf{z}} - \mathbf{B}\hat{\mathbf{z}} = \mathbf{0}, \quad (4)$$

and, as a consequence, the corresponding state equation in the time-domain contains one-half derivatives due to the power 1/2 of Ω in the frequency domain. Such derivatives have been treated in mathematics, and are called

1 fractional derivatives. A recent paper on this matter, involving diffusion with
 2 fractional derivatives, has been published by Birk and Song [6]. There, too,
 3 problems from numerical noise have to be treated by using spectral shifting
 4 with deflation.

5 The paper is organized as follows: in Section 2 the essentials of deflation
 6 and eigenvalue-shifting are repeated and prepared for Section 3, where it will
 7 be shown how the loss of sparsity of state-space matrix \mathbf{B} can be avoided by
 8 using a Sherman-Morrison like procedure.

9 This rather famous algorithm, which was developed in 1950 by Sher-
 10 man and Morrison (see [7]), and is well documented in [8], has been sub-
 11 sequently used both in several branches of mathematics (e.g. [9], [10], [11],
 12 [12], [13], [14], [15], [16], [17], [18], [19], [20]) and of applied mechanics ([21],
 13 [22], [23]); in particular, with reference to system-identification and system-
 14 modification, typical examples can be found in [24], [25] and [26].

15 Finally in Section 4 an example from soil-structure interaction, including
 16 wave propagation due to an unbounded soil domain, shows the effectiveness
 17 of the procedure presented in this paper.

18 A Sherman-Morrison like treatment of linear algebraic equations is partic-
 19 ularly useful when dealing with time-solvers with time-step control and thus
 20 with a continuously changing coefficient matrix. Moreover it can be advanta-
 21 geously adopted in several other mechanical problems, especially when only
 22 a small part of system matrices coefficients is going to experience changes
 23 due to time evolution, but such changes are able to destroy the original pat-
 24 tern (whether banded, or tri-diagonal, or more generally sparse) of matrix
 25 structure.

26 Among these problems, the following ones can be mentioned:

- 27 • dynamical system identification under special conditions (see, e.g. [27],
 28 [28], [29]);
- 29 • dynamical problems with functionally-graded materials or surface stresses
 30 (viz. [30], [31]);
- 31 • structural dynamics for special loading conditions (like, for instance,
 32 galloping [32] or moving loads [33], [34], [35]);
- 33 • wave propagation in non-classical continua ([36], [37], [38], [39]);
- 34 • remodeling and evolution problems in biomechanics (see, for instance,
 35 [40], [41], [42]).

2. Deflation, Eigenvalue Shifting

The SBFEM is a powerful method in order to model unbounded domains. It is a semi-analytical method which solves the problem in the unbounded direction analytically. Typical outcome of the SBFEM is a finite set of impedances $K_c(\lambda_j)$ for discrete values $\lambda = i\Omega$; here Ω is used as usual instead of β . These samples are taken to establish a rational interpolation like (3) or a corresponding continued fractions realization (the one, which is shown here, holds for $M = 4$):

$$\hat{f}_c = K_c \hat{u}_c,$$

$$K_c = S_c + \lambda T_c - \frac{C_c^2}{S_1 + \lambda T_1 - \frac{C_1^2}{S_2 + \lambda T_2 - \frac{C_2^2}{S_3 + \lambda T_3 - \frac{C_3^2}{S_4 + \lambda T_4}}}}. \quad (5)$$

In(5) the coefficients S_j, T_j, C_k ($j = c, 1, \dots, M; k = c, 1, \dots, M - 1$) can be taken to establish a corresponding tridiagonal state-space formulation. For the sake of simplicity here the rational interpolation as well as the continued fractions realization refer to a Single-Input, Single-Output (SISO) problem.

The nonlinear continued fractions realization can be rewritten in a formal linear manner by introducing internal variables v_j . The outcome is shown in (6) where in parallel the step from SISO- to MIMO-systems (i.e. Multiple-Input, Multiple-Output) has been done by simply changing from scalar quantities to matrix-valued ones, again for the case $M = 4$:

$$\lambda \mathbf{A} \hat{\mathbf{z}} - \mathbf{B} \hat{\mathbf{z}} = \hat{\mathbf{f}}, \quad \hat{\mathbf{z}} = \begin{bmatrix} \hat{\mathbf{u}}_c \\ \hat{\mathbf{v}}_1 \\ \hat{\mathbf{v}}_2 \\ \hat{\mathbf{v}}_3 \\ \hat{\mathbf{v}}_4 \end{bmatrix}, \quad \hat{\mathbf{f}} = \begin{bmatrix} \hat{\mathbf{f}}_c \\ \mathbf{0} \\ \mathbf{0} \\ \mathbf{0} \\ \mathbf{0} \end{bmatrix}, \quad (6)$$

$$\mathbf{A} = \begin{bmatrix} \mathbf{T}_c & \mathbf{0} & \mathbf{0} & \mathbf{0} & \mathbf{0} \\ \mathbf{0} & -\mathbf{T}_1 & \mathbf{0} & \mathbf{0} & \mathbf{0} \\ \mathbf{0} & \mathbf{0} & \mathbf{T}_2 & \mathbf{0} & \mathbf{0} \\ \mathbf{0} & \mathbf{0} & \mathbf{0} & -\mathbf{T}_3 & \mathbf{0} \\ \mathbf{0} & \mathbf{0} & \mathbf{0} & \mathbf{0} & \mathbf{T}_4 \end{bmatrix}, \quad (7)$$

$$\mathbf{B} = \begin{bmatrix} -\mathbf{S}_c & -\mathbf{C}_c & \mathbf{0} & \mathbf{0} & \mathbf{0} \\ -\mathbf{C}_c^T & \mathbf{S}_1 & \mathbf{C}_1 & \mathbf{0} & \mathbf{0} \\ \mathbf{0} & \mathbf{C}_1^T & -\mathbf{S}_2 & -\mathbf{C}_2 & \mathbf{0} \\ \mathbf{0} & \mathbf{0} & -\mathbf{C}_2^T & \mathbf{S}_3 & \mathbf{C}_3 \\ \mathbf{0} & \mathbf{0} & \mathbf{0} & \mathbf{C}_3^T & -\mathbf{S}_4 \end{bmatrix}. \quad (8)$$

1 By eliminating the quantities v_4 down to v_1 the original nonlinear continued
 2 fractions realization can be recovered. This process with internal variables,
 3 ending with a state-space formulation in the time-domain:

$$\mathbf{A}\mathbf{z} - \mathbf{B}\mathbf{z} = \mathbf{f}, \quad \mathbf{z} = \hat{\mathbf{z}} \exp(\lambda t), \quad \lambda = \alpha + i\beta, \quad (9)$$

4 is characterized by a block-diagonal matrix \mathbf{A} multiplied with λ and a block-
 5 tridiagonal matrix \mathbf{B} .

6 Obviously there are strong relations between the rational interpolation (3),
 7 the continued fractions (5) and the system of Ordinary Differential Equations
 8 (ODEs) (9) with sparse matrices. In other words, if a problem can be mod-
 9 eled in a rational manner or by continued fractions, it belongs to the class of
 10 systems with a tridiagonal matrix representation. All this is well-known and
 11 described in textbooks like [43].

12 As it has been already mentioned, the stability of the coupled system (5)
 13 can be contaminated by numerical noise hidden in finding the coefficients
 14 P_j, Q_j or $\mathbf{S}_j, \mathbf{T}_j, \mathbf{C}_k$ by a least-square approach.

15 In [44] Du and Zhao tried to avoid *a priori* spurious eigenvalues, by com-
 16 bining the least-square-approach with the constraint $\text{Re}(\lambda) \leq 0$. However,
 17 the convergence of this process is rather poor and it has, so far, been applied
 18 only to systems with one original degree of freedom.

19 Thus, in the present case, stability is established *a posteriori*. This can be
 20 done either by eliminating the spurious modes by means of modal reduction
 21 or by spectral shifting. In the latter case, the full original solution space is
 22 maintained and therefore this method has been chosen here.

23 All eigenvalues $\lambda = \alpha + i\beta$ with positive real part (i.e. with $\alpha > 0$) are
 24 simply shifted to the left side of the complex plane to become $\tilde{\lambda}$ with a
 25 negative real part, so that $\tilde{\alpha} \leq 0$, and with an unchanged imaginary part, β :

$$\lambda = \alpha + i\beta \quad \text{with } \alpha > 0 \Rightarrow \tilde{\lambda} = \tilde{\alpha} + i\beta \quad \text{with } \tilde{\alpha} \leq 0. \quad (10)$$

This process needs all eigenvectors (the left ones, \mathbf{y} , and the right ones, \mathbf{x}), related to the eigenvalues λ whose real part, α is positive. If any λ_j is complex, $\lambda_j = \alpha_j + i\beta_j$, that means automatically that its complex conjugate, $\bar{\lambda}_j = \alpha_j - i\beta_j$ is also an eigenvalue (and for a better organization it will be labeled as λ_{j+1}), the corresponding eigenvectors $\mathbf{x}_j = \mathbf{a}_j \pm i\mathbf{b}_j$, $\mathbf{y}_j = \mathbf{u}_j \pm i\mathbf{v}_j$ are stored in a pairwise and real-valued form,

$$\mathbf{P}_j = [\mathbf{a}_j \quad \mathbf{b}_j], \quad \mathbf{Q}_j = [\mathbf{u}_j \quad \mathbf{v}_j], \quad (11)$$

and used to shift the real part α to $\tilde{\alpha} = \alpha - \epsilon$ by modal deflation of the system matrix \mathbf{B} to $\tilde{\mathbf{B}}$.

The original right- and left-eigenproblems:

$$\lambda \mathbf{A} \mathbf{x} = \mathbf{B} \mathbf{x}; \quad \lambda \mathbf{A}^T \mathbf{y} = \mathbf{B}^T \mathbf{y}, \quad (12)$$

become after deflation:

$$\tilde{\lambda} \mathbf{A} \mathbf{x} = \tilde{\mathbf{B}} \mathbf{x}; \quad \tilde{\lambda} \mathbf{A}^T \mathbf{y} = \tilde{\mathbf{B}}^T \mathbf{y} \quad \text{with } \tilde{\lambda} = \lambda - \epsilon; \quad (13)$$

where the right- and left-eigenvectors are the *same* in both cases, (12) and (13).

When there is a complex conjugate pair of eigenvalues $\lambda_j = \alpha + i\beta$, $\lambda_{j+1} = \alpha - i\beta$ with the *same* $\alpha > 0$ and β , then a *rank-two modification* leads to

$$\tilde{\mathbf{B}} = \mathbf{B} - \epsilon \mathbf{A} \mathbf{P}_j (\mathbf{Q}_j^T \mathbf{A} \mathbf{P}_j)^{-1} \mathbf{Q}_j^T \mathbf{A}, \quad (14)$$

where, $\mathbf{Q}_j^T \mathbf{A} \mathbf{P}_j$ is a 2×2 matrix which can be inverted explicitly.

If, instead, the eigenvalue $\lambda_j = \alpha > 0$ is a pure real number (i.e. $\beta = 0$), then the corresponding eigenvector is real too, $\mathbf{x}_j = \mathbf{a}$, $\mathbf{y}_j = \mathbf{u}$ and it comes out that

$$\tilde{\mathbf{B}} = \mathbf{B} - \epsilon \mathbf{A} \mathbf{x}_j (\mathbf{y}_j^T \mathbf{A} \mathbf{x}_j)^{-1} \mathbf{y}_j^T \mathbf{A}, \quad (15)$$

contains the inverse of a scalar. The procedure shown in (15) is called a *rank-one modification*.

The theory behind these equations traces back to a real-valued modal decoupling where the n_c pairs of conjugate complex eigenvectors are assembled pairwise and real-valued by means of \mathbf{P}_j or \mathbf{Q}_j , followed by the $n_r = N - 2n_c$

1 remaining real eigenvectors \mathbf{x}_j or \mathbf{y}_j , to produce suitable $N \times N$ square ma-
 2 trices \mathbf{Y} and \mathbf{X} with real entries:

$$\mathbf{Y} = [\mathbf{Q}_1 \cdots \mathbf{Q}_{n_c} \quad \mathbf{y}_1 \cdots \mathbf{y}_{n_r}], \quad (16)$$

$$\mathbf{X} = [\mathbf{P}_1 \cdots \mathbf{P}_{n_c} \quad \mathbf{x}_1 \cdots \mathbf{x}_{n_r}], \quad (17)$$

3 where $N = 2n_c + n_r$ is the total number of eigenvalues.

4 Then it follows that:

$$\mathbf{Y}^T \mathbf{A} \mathbf{X} = \begin{bmatrix} \mathbf{A}_{11} & \cdots & \mathbf{0} & \mathbf{0} & \cdots & \mathbf{0} \\ \vdots & \ddots & \vdots & \vdots & \ddots & \vdots \\ \mathbf{0} & \cdots & \mathbf{A}_{n_c, n_c} & \mathbf{0} & \cdots & \mathbf{0} \\ \mathbf{0} & \cdots & \mathbf{0} & a_1 & \cdots & 0 \\ \vdots & \cdots & \vdots & \vdots & \ddots & \vdots \\ \mathbf{0} & \cdots & \mathbf{0} & 0 & \cdots & a_{n_r} \end{bmatrix}, \quad (18)$$

$$\mathbf{Y}^T \mathbf{B} \mathbf{X} = \begin{bmatrix} \mathbf{B}_{11} & \cdots & \mathbf{0} & \mathbf{0} & \cdots & \mathbf{0} \\ \vdots & \ddots & \vdots & \vdots & \ddots & \vdots \\ \mathbf{0} & \cdots & \mathbf{B}_{n_c, n_c} & \mathbf{0} & \cdots & \mathbf{0} \\ \mathbf{0} & \cdots & \mathbf{0} & b_1 & \cdots & 0 \\ \vdots & \cdots & \vdots & \vdots & \ddots & \vdots \\ \mathbf{0} & \cdots & \mathbf{0} & 0 & \cdots & b_{n_r} \end{bmatrix}, \quad (19)$$

5 where \mathbf{A}_{jj} and \mathbf{B}_{jj} (with $j = 1, \dots, n_c$) are 2×2 square matrices; a_l, b_l (with
 6 $l = 1, \dots, n_r$) are real scalar values; while all matrices and vectors \mathbf{X}, \mathbf{Y} ,
 7 $\mathbf{A}_{jj}, \mathbf{B}_{jj}, \mathbf{a}_j, \mathbf{b}_j, \mathbf{u}_j, \mathbf{v}_j \in \mathbb{R}$.

8 Moreover,

$$\mathbf{A}_{jj} = \mathbf{Q}_j \mathbf{A} \mathbf{P}_j = \begin{bmatrix} \mathbf{u}_j^T \\ \mathbf{v}_j^T \end{bmatrix} \mathbf{A} [\mathbf{a}_j \quad \mathbf{b}_j] = \begin{bmatrix} \mathbf{u}_j^T \mathbf{A} \mathbf{a}_j & \mathbf{u}_j^T \mathbf{A} \mathbf{b}_j \\ \mathbf{v}_j^T \mathbf{A} \mathbf{a}_j & \mathbf{v}_j^T \mathbf{A} \mathbf{b}_j \end{bmatrix}. \quad (20)$$

$$\mathbf{B}_{jj} = \mathbf{Q}_j \mathbf{B} \mathbf{P}_j = \begin{bmatrix} \mathbf{u}_j^T \\ \mathbf{v}_j^T \end{bmatrix} \mathbf{B} [\mathbf{a}_j \quad \mathbf{b}_j] = \begin{bmatrix} \mathbf{u}_j^T \mathbf{B} \mathbf{a}_j & \mathbf{u}_j^T \mathbf{B} \mathbf{b}_j \\ \mathbf{v}_j^T \mathbf{B} \mathbf{a}_j & \mathbf{v}_j^T \mathbf{B} \mathbf{b}_j \end{bmatrix}. \quad (21)$$

9 This pairwise assembling (11) avoids the use of complex numbers.

10 If complex eigenvectors $\tilde{\mathbf{x}}_j, \tilde{\mathbf{y}}_j$ are instead used, complex bilinear quan-
 11 tities \tilde{a}_j and \tilde{b}_j result, which lead directly to the corresponding eigenvalue
 12 λ :

$$\tilde{\mathbf{y}}_j^T \mathbf{A} \tilde{\mathbf{x}}_j = a_j, \quad \tilde{\mathbf{y}}_j^T \mathbf{B} \tilde{\mathbf{x}}_j = b_j; \quad \lambda_j = \frac{b_j}{a_j}, \quad (22)$$

where $\tilde{\mathbf{x}}_j, \tilde{\mathbf{y}}_j, \tilde{a}_j, \tilde{b}_j \in \mathbb{C}$.

As it can be easily checked, both approach, with complex conjugate eigenvectors stored as contiguous real arrays (11), leading to (18)–(19), and with complex variables, produce the same results, i.e. (20)–(21) and (22) are confirmed.

It is useful noticing that most eigenvalue solvers which are available for dealing with real matrices take advantage of the property that for a square matrix with real entries, its complex eigenvalues (if any) will always occur in complex conjugate pairs, and this holds also for the corresponding eigenvectors. As a consequence, both eigenvalues (similar considerations apply to eigenvectors, too) belonging to the *same* conjugate pair are completely known if their real part and the imaginary part of just *one element of the pair* are given.

This properties suggests saving memory-allocation space by storing eigenvalues (or eigenvectors) in contiguous locations, reserving the first location for the real part and the second for the imaginary part which characterize completely the complex conjugate pair.

This kind of storage scheme is adopted, for instance, by the eigenvalue solver **RGG** belonging to the **EISPACK** [45] package or by **DGGEVX** being part of the **LAPACK** [46] package: they end up with eigenvectors which are ordered as real pairs \mathbf{Q}_j -wise and \mathbf{P}_j -wise, so that (20)–(21) apply.

Multiplying the modified matrix $\tilde{\mathbf{B}}$ in (15), from the left side with the pair \mathbf{Q}_j of left-eigenvectors, and from the right side with the pair \mathbf{P}_j of right-eigenvectors, activates the shifted part with the same index j , including ϵ .

A similar multiplication, but now with a different pair $\mathbf{Q}_k, \mathbf{P}_k$ than that in the ϵ -part does not activate the modification, due to the orthogonality condition $\mathbf{Q}_k^T \mathbf{A} \mathbf{P}_j = \mathbf{0}$, $\mathbf{Q}_k^T \mathbf{B} \mathbf{P}_j = \mathbf{0}$.

Indeed, by properties of deflation, it follows:

$$\tilde{\lambda} \mathbf{A} \mathbf{x} = \tilde{\mathbf{B}} \mathbf{x}; \quad \tilde{\lambda} \mathbf{A}^T \mathbf{y} = \tilde{\mathbf{B}}^T \mathbf{y}. \quad (23)$$

Hence, in the former case, i.e. when the *same* pair $\mathbf{Q}_j, \mathbf{P}_j$ of left- and right-eigenvector is involved, it results

$$\mathbf{Q}_j^T \mathbf{A} \mathbf{P}_j = \mathbf{A}_{jj}, \quad (24)$$

$$\mathbf{Q}_j^T \tilde{\mathbf{B}} \mathbf{P}_j = \mathbf{Q}_j^T [\mathbf{B} - \epsilon \mathbf{A} \mathbf{P}_j (\mathbf{Q}_j^T \mathbf{A} \mathbf{P}_j)^{-1} \mathbf{Q}_j^T \mathbf{A}] \mathbf{P}_j = \mathbf{B}_{jj} - \epsilon \mathbf{A}_{jj}. \quad (25)$$

1 In the latter case, when a *different* pair of eigenvectors is dealt with, it comes
2 out:

$$\mathbf{Q}_k^T \mathbf{A} \mathbf{P}_k = \mathbf{A}_{kk}, \quad (26)$$

$$\mathbf{Q}_k^T \tilde{\mathbf{B}} \mathbf{P}_k = \mathbf{Q}_k^T [\mathbf{B} - \epsilon \mathbf{A} \mathbf{P}_j (\mathbf{Q}_j^T \mathbf{A} \mathbf{P}_j)^{-1} \mathbf{Q}_j^T \mathbf{A}] \mathbf{P}_k = \mathbf{B}_{kk} - \epsilon \mathbf{0}. \quad (27)$$

3 Thus, it follows $\tilde{\lambda}_k = \lambda_k$ for $k \neq j$; $\tilde{\lambda}_j = \lambda_j - \epsilon$.

4 3. Numerical treatment of the modified matrix $\tilde{\mathbf{B}}$

5 The solution of the resulting equation of motion, a first-order ODE:

$$\mathbf{A} \dot{\mathbf{z}} = \tilde{\mathbf{B}} \mathbf{z} + \mathbf{f}, \quad (28)$$

6 where $\tilde{\mathbf{B}}$ is the modified system matrix coming out at the end of the deflation
7 procedure, is performed by means of a linear interpolation:

$$\mathbf{z} = \mathbf{z}_{k-1} \left(1 - \frac{\tau}{h}\right) + \mathbf{z}_k \frac{\tau}{h} \quad (29)$$

8 within a local time-interval $0 \leq \tau \leq h$ followed by an integration within this
9 interval.

10 This is an *a priori* stable process with a local error proportional to the
11 third power of the time-step as it has been shown, for example, in [47].

12 The resulting equation for a time-step between time-nodes $k-1$ and k
13 contains $\tilde{\mathbf{B}}$ on both sides of the linear algebraic equation:

$$\left(\mathbf{A} - \frac{h}{2} \tilde{\mathbf{B}}\right) \mathbf{z}_k = \left(\mathbf{A} + \frac{h}{2} \tilde{\mathbf{B}}\right) \mathbf{z}_{k-1} + \int_{k-1}^k \mathbf{f}(t) dt, \quad (30)$$

14 where matrices \mathbf{A} and \mathbf{B} (the original one, not the modified $\tilde{\mathbf{B}}$), are given,
15 for the case $M = 5$ (this is an example: a comparison with (7)–(8), where M
16 is even, may be useful), by:

$$\mathbf{A} = \begin{bmatrix} \mathbf{T}_c & \mathbf{0} & \mathbf{0} & \mathbf{0} & \mathbf{0} & \mathbf{0} \\ \mathbf{0} & -\mathbf{T}_1 & \mathbf{0} & \mathbf{0} & \mathbf{0} & \mathbf{0} \\ \mathbf{0} & \mathbf{0} & \mathbf{T}_2 & \mathbf{0} & \mathbf{0} & \mathbf{0} \\ \mathbf{0} & \mathbf{0} & \mathbf{0} & -\mathbf{T}_3 & \mathbf{0} & \mathbf{0} \\ \mathbf{0} & \mathbf{0} & \mathbf{0} & \mathbf{0} & \mathbf{T}_4 & \mathbf{0} \\ \mathbf{0} & \mathbf{0} & \mathbf{0} & \mathbf{0} & \mathbf{0} & -\mathbf{T}_5 \end{bmatrix}, \quad (31)$$

$$\mathbf{B} = \begin{bmatrix} -\mathbf{S}_c & -\mathbf{C}_c & \mathbf{0} & \mathbf{0} & \mathbf{0} & \mathbf{0} \\ -\mathbf{C}_c^T & \mathbf{S}_1 & \mathbf{C}_1 & \mathbf{0} & \mathbf{0} & \mathbf{0} \\ \mathbf{0} & \mathbf{C}_1^T & -\mathbf{S}_2 & -\mathbf{C}_2 & \mathbf{0} & \mathbf{0} \\ \mathbf{0} & \mathbf{0} & -\mathbf{C}_2^T & \mathbf{S}_3 & \mathbf{C}_3 & \mathbf{0} \\ \mathbf{0} & \mathbf{0} & \mathbf{0} & \mathbf{C}_3^T & -\mathbf{S}_4 & -\mathbf{C}_4 \\ \mathbf{0} & \mathbf{0} & \mathbf{0} & \mathbf{0} & -\mathbf{C}_4^T & \mathbf{S}_5 \end{bmatrix}, \quad (32)$$

Matrices \mathbf{A} and \mathbf{B} in (31)–(32) are block-diagonal ones; however, this property is lost when \mathbf{B} is replaced by $\tilde{\mathbf{B}}$ following the deflation process: for instance, with a *rank-2 complement*, see (14), if one complex eigensolution is deflated, or with a rank-1 complement, see (15), for a single real eigensolution.

Nevertheless, the decomposition of the fully filled matrix $[\mathbf{A} - \frac{h}{2}\tilde{\mathbf{B}}]$ can be avoided and replaced by the decomposition of the original pair $[\mathbf{A} - \frac{h}{2}\mathbf{B}]$.

Indeed, taking into account (14) or (15) the left-hand side of the modified problem (30) used to compute the solution at time-node k , once the solution at time-node $k - 1$ is known, can be rewritten in this form:

$$[\mathbf{A} - \frac{h}{2}\tilde{\mathbf{B}}]\mathbf{z}_k = [\mathbf{A} - \frac{h}{2}\mathbf{B} - \frac{h}{2}\sum_{j=1}^{n_s} \mathbf{L}_j \mathbf{R}_j^T]\mathbf{z}_k = \mathbf{f}_k; \quad (33)$$

$$\mathbf{f}_k = [\mathbf{A} + \frac{h}{2}\tilde{\mathbf{B}}]\mathbf{z}_{k-1} + \int_{k-1}^k \mathbf{f}(t)dt, \quad (34)$$

where the shortcut notation

$$\tilde{\mathbf{B}} = \mathbf{B} + \sum_{j=1}^{n_s} \mathbf{L}_j \mathbf{R}_j^T \quad (35)$$

has been employed, and $n_s = n_r^* + n_c^*$ is the number of deflation steps required to shift all eigenvalues (the n_r^* real ones and the n_c^* complex conjugate pairs) having a positive real part.

1 It can be easily checked that matrices \mathbf{L}_j and \mathbf{R}_j appearing in (35) are
 2 given, in the case of a pair of complex-conjugate eigenvalues by:

$$\mathbf{L}_j = -\epsilon \mathbf{A} \mathbf{P}_j (\mathbf{Q}_j^T \mathbf{A} \mathbf{P}_j)^{-1}, \quad \mathbf{R}_j = \mathbf{A}^T \mathbf{Q}_j, \quad (36)$$

3 while in the case of a real eigenvalue they are simply:

$$\mathbf{L}_j = -\epsilon \mathbf{A} \mathbf{x}_j (\mathbf{y}_j^T \mathbf{A} \mathbf{x}_j)^{-1}, \quad \mathbf{R}_j = \mathbf{A}^T \mathbf{y}_j, \quad (37)$$

4 For the subsequent developments, it is useful noticing that, taking into ac-
 5 count the properties of matrix addition and multiplication, the cumulative
 6 effect of the deflation procedure can be written in this way, as a simple prod-
 7 uct of the two matrices \mathbf{L} and \mathbf{R} :

$$\sum_{j=1}^{n_s} \mathbf{L}_j \mathbf{R}_j^T = \mathbf{L} \mathbf{R}^T. \quad (38)$$

8 Matrices \mathbf{L} and \mathbf{R} are simply obtained by pulling together, column by column
 9 (in the *same* order) the \mathbf{L}_j and the \mathbf{R}_j matrices which appear in (36) or (37):

$$\mathbf{L} = [\mathbf{L}_1 \ \mathbf{L}_2 \ \cdots \ \mathbf{L}_{n_s}] = [\mathbf{l}_1 \ \cdots \ \mathbf{l}_{n_d}], \quad (39)$$

$$\mathbf{R} = [\mathbf{R}_1 \ \mathbf{R}_2 \ \cdots \ \mathbf{R}_{n_s}] = [\mathbf{r}_1 \ \cdots \ \mathbf{r}_{n_d}], \quad (40)$$

10 where $n_d = n_r^* + 2n_c^*$ is the total number of columns of matrices \mathbf{L} and \mathbf{R} .
 11 The procedure in order to solve problem (33)–(34) runs as follows:

- 12 1. *First step.* Solve the system of linear algebraic equations with the
 13 original (i.e. not deflated) tridiagonal matrix \mathbf{B} :

$$[\mathbf{A} - \frac{h}{2} \mathbf{B}] \mathbf{w} = \mathbf{f}_k \quad (41)$$

14 and save the value into an auxiliary variable \mathbf{w} .

- 15 2. *Second step.* With the amount of n_d right-hand sides \mathbf{l}_j solve the prob-
 16 lem:

$$[\mathbf{A} - \frac{h}{2} \mathbf{B}] \mathbf{x}_j^* = \mathbf{l}_j, \quad (j = 1, \dots, n_d) \quad (42)$$

17 collecting the results into matrix \mathbf{X}^* defined as:

$$\mathbf{X}^* = [\mathbf{x}_1^* \ \cdots \ \mathbf{x}_{n_d}^*]. \quad (43)$$

Actually, the sequence of computations performed in this step can be written synthetically as

$$\left[\left(\mathbf{A} - \frac{h}{2} \mathbf{B} \right) \right] \mathbf{X}^* = \mathbf{L}. \quad (44)$$

Since the solution of the linear algebraic system defined by (42) or (44) involves the *same* l.h.s. as (41), the decomposition of $\left[\mathbf{A} - \frac{h}{2} \mathbf{B} \right]$ can be performed only once in the first step and then used here, too.

3. *Third step.* Compute the solution \mathbf{z}_k at time node k with a suitable combination of the solutions \mathbf{w} , and \mathbf{X}^* :

$$\mathbf{z}_k = \mathbf{w} + \mathbf{X}^* \mathbf{c}; \quad \mathbf{c}^T = [c_1 \quad \cdots \quad c_{n_d}], \quad (45)$$

by solving the following system of linear algebraic equations:

$$\left[\mathbf{I} - \frac{h}{2} \mathbf{R}^T \mathbf{X}^* \right] \mathbf{c} = \frac{h}{2} \mathbf{R}^T \mathbf{w}, \quad (46)$$

which defines the n_d coefficients c_j ($j = 1, \dots, n_d$) of the linear combination (45). Thus, for instance, if only one real spurious eigenvalue has to be shifted, $n_d = 1$ and (46) becomes a scalar equation for c_1 . It is worth noticing that in (46) \mathbf{I} is an identity matrix of order n_d .

The correctness of this sequence can be checked by rewriting the original equation, see (33), $\left[\mathbf{A} - \frac{h}{2} \mathbf{B} \right] \mathbf{z}_k = \mathbf{f}_k$ by using $\mathbf{z}_k = \mathbf{w} + \mathbf{X}^* \mathbf{c}$:

$$\left[\left(\mathbf{A} - \frac{h}{2} \mathbf{B} \right) - \frac{h}{2} \mathbf{L} \mathbf{R}^T \right] [\mathbf{w} + \mathbf{X}^* \mathbf{c}] - \mathbf{f}_k = \mathbf{0}, \quad (47)$$

and taking into account that, by (41):

$$\left[\left(\mathbf{A} - \frac{h}{2} \mathbf{B} \right) \right] \mathbf{w} - \mathbf{f}_k = \mathbf{0}, \quad (48)$$

while, by (39) and (44), (47) becomes:

$$\mathbf{L} \left[\mathbf{c} - \frac{h}{2} \mathbf{R}^T (\mathbf{w} + \mathbf{X}^* \mathbf{c}) \right] = \mathbf{0}. \quad (49)$$

Now it is easy to distinguish within the square brackets of (49), with some rearrangements, the appearance of (46).

1 A simple example illustrating the basic steps of the procedure described
2 above is presented in Appendix A.

3 The evaluation of the term $(\mathbf{A} + \frac{h}{2}\tilde{\mathbf{B}})\mathbf{z}_{k-1}$ contributing to the right-hand
4 side \mathbf{f}_k —see (34)— should be organized in a numerically convenient way,
5 too, as it is shown in the following:

$$(\mathbf{A} + \frac{h}{2}\tilde{\mathbf{B}})\mathbf{z}_{k-1} = (\mathbf{A} + \frac{h}{2}\mathbf{B})\mathbf{z}_{k-1} + \frac{h}{2}\mathbf{L} [\mathbf{R}^T \mathbf{z}_{k-1}]. \quad (50)$$

6 Here, for a better memory allocation strategy, the product $\mathbf{p}^* = [\mathbf{R}^T \mathbf{z}_{k-1}]$
7 has to be calculated first, and only afterwards the matrix multiplication $\mathbf{L}\mathbf{p}^*$
8 has to be computed.

9 Another possible strategy to solve problem (33)–(34) without explicitly
10 using matrix $\tilde{\mathbf{B}}$ consists in adding the deflated part of \mathbf{B} by making use of
11 this larger partitioned matrix:

$$\begin{bmatrix} \mathbf{A} - \frac{h}{2}\mathbf{B} & \mathbf{L} \\ \frac{h}{2}\mathbf{R}^T & \mathbf{I} \end{bmatrix} \begin{bmatrix} \mathbf{z}_k \\ \mathbf{a}^* \end{bmatrix} = \begin{bmatrix} \mathbf{f}_k \\ \mathbf{0} \end{bmatrix}. \quad (51)$$

12 It is an easy task verifying that the solution of the system of linear algebraic
13 equations (51), when internal variables \mathbf{a}^* are statically condensed, is exactly
14 the same as that of system (33)–(34). However this formulation, even though
15 it is more compact and elegant, does not preserve the sparsity of the original
16 matrices \mathbf{A} and \mathbf{B} : therefore it requires a larger amount of memory and,
17 preventing the use of linear algebra tools which have been devised for banded
18 matrices, is less convenient from a computational point of view.

19 4. Example: Rotor on unbounded soil-domain during short-circuit 20 torque excitation

21 A soil-foundation-rotor interaction problem shown in Figure 1 is used
22 in order to demonstrate the procedure and to count the global amount of
23 operations when taking care for the banded matrices.

24 The foundation is modeled as a perfectly rigid one; thus in a section plane
25 there are only three degrees-of-freedom (DOFs): the vertical displacement
26 w , the horizontal displacement u , and the rocking rotation φ . The angle φ
27 is multiplied with a characteristic length, L like φL with $L = 5$ m, in order
28 to have DOFs with common physical dimensions. Here, only the coupled
29 horizontal and rocking motions (u and φL) will be considered, while the

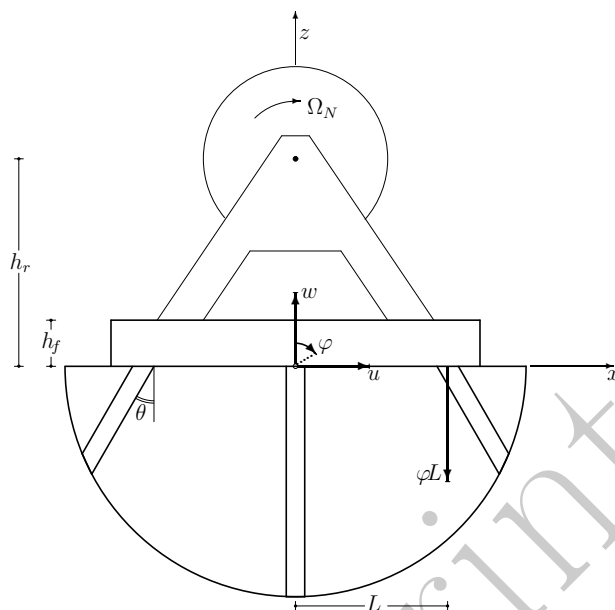


Figure 1: A sketch of the problem: a rotor supported by a slab foundation on inclined piles.

vertical motion w , which is decoupled, can be studied separately as a single DOF system.

In electrical engineering, the short-circuit torque of machines is a critical event and has to be studied. In situations, where precise machine-data are not available, the German code DIN 4024 (Foundations of machines) [48] presents this estimate for the torque:

$$M_{sc}(t) = -M_0 + 10M_0 \exp\left(\frac{-t}{0.4}\right) \left[\sin(\Omega_N t) - \frac{1}{2} \sin(2\Omega_N t) \right] + M_0 \exp\left(\frac{-t}{0.15}\right). \quad (52)$$

In (52), whose time evolution is plotted in Figure 2, time is denoted by t , and must be expressed in s; Ω_N is the nominal angular frequency of the machine and M_0 is the available nominal bracing-moment.

For the considered problem and taking into account Figure 1 for the meaning of the adopted symbols, the following input data set has been used: height of rotor axis with reference to contact point with soil, $h_r = 5$ m; foundation thickness, $h_f = 0.4$ m; rotor mass, $m_r = 6000$ kg; rotor moment of inertia with respect to contact point with soil, $J_r = 196,000$ kg·m²; founda-

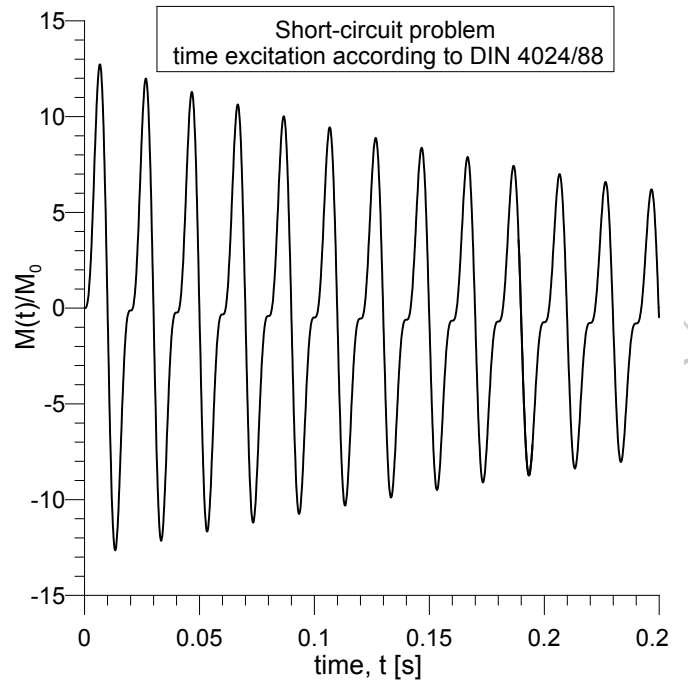


Figure 2: Prescribed time evolution of the short-circuit torque according to German code DIN 4024 (Foundations for machines) [48].

1 tion mass (excluding rotor), $m_f = 18,000$ kg; foundation moment of inertia
 2 (excluding rotor) with respect to contact point with soil, $J_f = 54,960$ kg·m²;
 3 bracing moment, $M_0 = 1,000,000$ N·m; nominal angular frequency of the
 4 machine, $\Omega_N = 78.53982$ rad/s.

5 The soil is modeled as a half-space as well as a stratum on bedrock. The
 6 dynamic stiffness of the soil in the frequency-domain has been transferred to
 7 the time-domain in [49] by a rational approximation and the same data are
 8 used here: in particular, for the Padé rational approximation an order $M = 7$

in the nominator and $M + 1 = 8$ in the denominator has been adopted. 1

The dynamic stiffness coefficients K_{hh} , $K_{hrL} = K_{rLh}$, K_{rLrL} : 2

$$\begin{bmatrix} \hat{f}_u \\ \hat{f}_{\varphi L} \end{bmatrix} = \begin{bmatrix} K_{hh} & K_{hrL} \\ K_{rLh} & K_{rLrL} \end{bmatrix} \begin{bmatrix} \hat{u} \\ \hat{\varphi}L \end{bmatrix}. \quad (53)$$

in the frequency-domain are those taken from [49] and are shown in Figures 3, 4 and 5. 3
4

In the time-domain the generalized forces $f_u, f_{\varphi L}$ in the interface are described by means of a first-order ODE with additional internal DOFs \mathbf{z}_f : 5
6

$$\mathbf{A} \begin{bmatrix} \dot{u} \\ \dot{\varphi}L \\ \dot{\mathbf{z}}_f \end{bmatrix} - \mathbf{B} \begin{bmatrix} u \\ \varphi L \\ \mathbf{z}_f \end{bmatrix} = \begin{bmatrix} f_u \\ f_{\varphi L} \\ \mathbf{0} \end{bmatrix}. \quad (54)$$

As already mentioned in Section 1, \mathbf{A} is a block-diagonal matrix and \mathbf{B} is block-tridiagonal. For the coupled horizontal-rocking motion of the foundation plate each block is a 2×2 matrix. 7
8
9

From the side of the foundation-plate with the rotor the equations of motion with respect to the coupling interface contain the generalized coupling forces $f_u, f_{\varphi L}$ as well, but with opposite sign. 10
11
12

$$\begin{aligned} m_r(\ddot{u} + \ddot{\varphi}h_r) + m_f(\ddot{u} + \ddot{\varphi}h_f/2) &= -f_u, \\ m_r(\ddot{u} + \ddot{\varphi}h_r)h_r + m_f(\ddot{u} + \ddot{\varphi}h_f/2)h_f/2 + (J_f + J_r)\ddot{\varphi} &= -f_{\varphi}, \end{aligned}$$

where $f_{\varphi L} = f_{\varphi}/L$ and m_r, m_f, J_r, J_f denote, respectively, the mass of the rotor and of the foundation and the mass-moment of inertia of the rotor and of the foundation, both measured with reference to the origin of the reference system. 13
14
15
16

An inertia matrix $\mathbf{J} = \mathbf{J}^T$ is defined in the following way: 17

$$\mathbf{J} = \begin{bmatrix} m_r + m_f & S_t \\ S_t & J_r + J_f \end{bmatrix},$$

altogether with $S_t = [m_r h_r + m_f h_f/2]/L$, denoting the total first-order mass moment. Hence, inertia forces can be given this expression: 18
19

$$\begin{bmatrix} -f_u \\ -f_{\varphi L} \end{bmatrix} = \mathbf{J} \begin{bmatrix} \ddot{u} \\ L\ddot{\varphi} \end{bmatrix}.$$

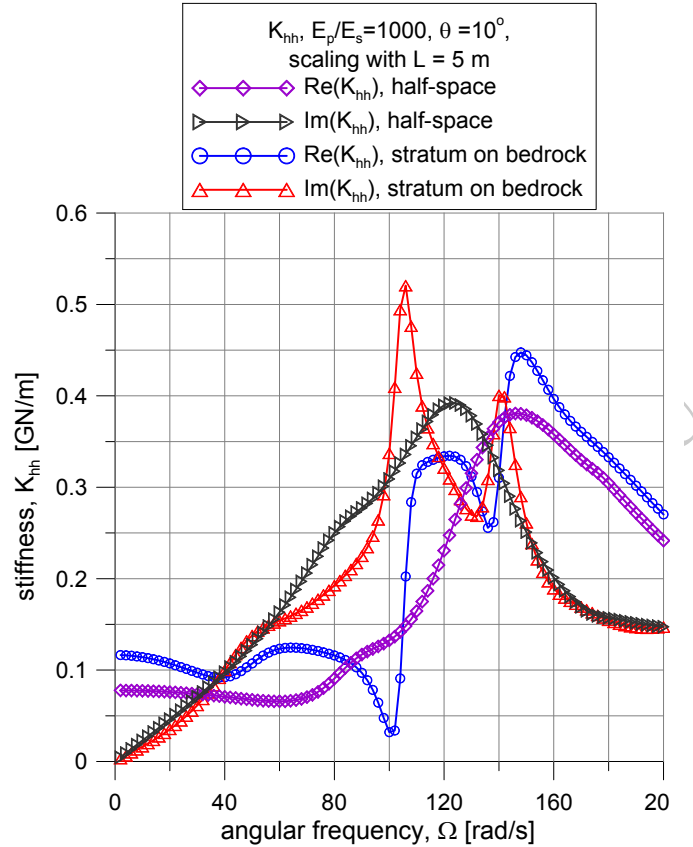


Figure 3: Complex stiffness modeled as a function of the angular frequency Ω : horizontal stiffness coefficient K_{hh} , for order of Padé's approximation $M = 7$. Hollow marks denote the assigned values, elaborated from [50] when piles are inclined at 10° . Real and imaginary part of stiffness are plotted for both cases of stratum on bedrock and of elastic half-space.

- 1 In order to describe the whole coupled soil-foundation-rotor problem the
- 2 equations of motion for the rotor plus foundation system are converted into
- 3 a system of first-order ODE by introducing the additional state-variables
- 4 $v_x = \dot{u}$ and $\omega L = \dot{\varphi}L$:

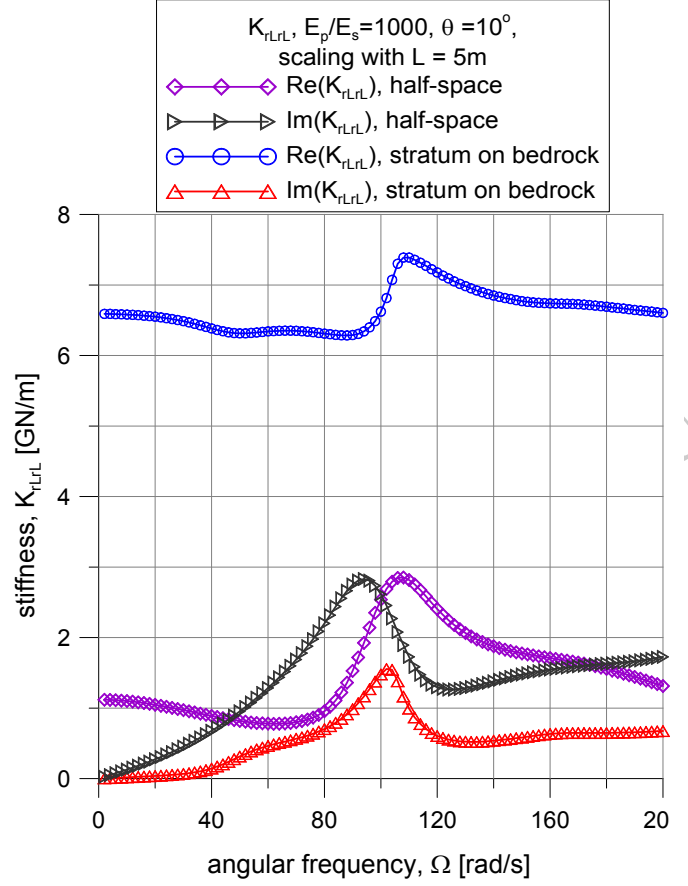


Figure 4: Complex stiffness modeled as a function of the angular frequency Ω : rocking stiffness coefficient K_{rLrL} , for order of Padé's approximation $M = 7$. Hollow marks denote the assigned values, elaborated from [50] when piles are inclined at 10° . Real and imaginary part of stiffness are plotted for both cases of stratum on bedrock and of elastic half-space.

$$\begin{bmatrix} \mathbf{0}_2 & \mathbf{J} \\ \mathbf{J} & \mathbf{0}_2 \end{bmatrix} \begin{bmatrix} \dot{v}_x \\ \dot{\omega}L \\ \dot{u} \\ \dot{\varphi}L \end{bmatrix} - \begin{bmatrix} \mathbf{J} & \mathbf{0}_2 \\ \mathbf{0}_2 & \mathbf{0}_2 \end{bmatrix} \begin{bmatrix} v_x \\ \omega L \\ u \\ \varphi L \end{bmatrix} = \begin{bmatrix} 0 \\ 0 \\ 0 \\ M_{sc}(t)/L \end{bmatrix} - \begin{bmatrix} 0 \\ 0 \\ f_u \\ f_{\varphi L} \end{bmatrix}. \quad (55)$$

Here $\mathbf{0}_2$ denotes a 2×2 null matrix; the torque $M_{sc}(t)$ caused by short-circuit 1

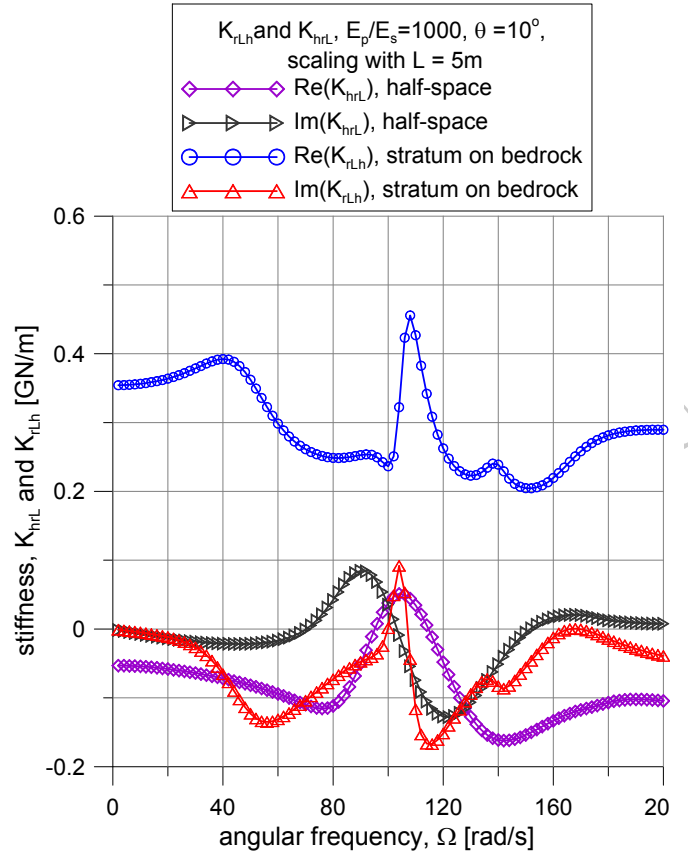


Figure 5: Complex stiffness modeled as a function of the angular frequency Ω : coupled horizontal-rocking stiffness coefficient K_{hrL} , for order of Padé's approximation $M = 7$. Hollow marks denote the assigned values, elaborated from [50] when piles are inclined at 10° . Real and imaginary part of stiffness are plotted for both cases of stratum on bedrock and of elastic half-space.

- 1 has been added to the right-hand side. These equations represent together
- 2 the complete coupled problem,

$$\mathbf{A}_{cc}\dot{\mathbf{z}} - \mathbf{B}_{cc}\mathbf{z} = \mathbf{f}, \quad (56)$$

- 3 where \mathbf{A}_{cc} , \mathbf{B}_{cc} , $\dot{\mathbf{z}}$, \mathbf{z} and \mathbf{f} are defined in the following way:

$$\mathbf{A}_{cc} = \left[\begin{array}{c|ccccccc} \mathbf{0}_2 & \mathbf{J} & \mathbf{0}_2 & \mathbf{0}_2 & \cdots & \mathbf{0}_2 & \mathbf{0}_2 & \mathbf{0}_2 \\ \hline \mathbf{J}^T & \mathbf{A}_0 & \mathbf{0}_2 & \mathbf{0}_2 & \cdots & \mathbf{0}_2 & \mathbf{0}_2 & \mathbf{0}_2 \\ \mathbf{0}_2 & \mathbf{0}_2 & \mathbf{A}_1 & \mathbf{0}_2 & \cdots & \mathbf{0}_2 & \mathbf{0}_2 & \mathbf{0}_2 \\ \mathbf{0}_2 & \mathbf{0}_2 & \mathbf{0}_2 & \mathbf{A}_2 & \cdots & \mathbf{0}_2 & \mathbf{0}_2 & \mathbf{0}_2 \\ \vdots & \vdots & \vdots & \vdots & \ddots & \vdots & \vdots & \vdots \\ \mathbf{0}_2 & \mathbf{0}_2 & \mathbf{0}_2 & \mathbf{0}_2 & \cdots & \mathbf{A}_{M-2} & \mathbf{0}_2 & \mathbf{0}_2 \\ \mathbf{0}_2 & \mathbf{0}_2 & \mathbf{0}_2 & \mathbf{0}_2 & \cdots & \mathbf{0}_2 & \mathbf{A}_{M-1} & \mathbf{0}_2 \\ \mathbf{0}_2 & \mathbf{0}_2 & \mathbf{0}_2 & \mathbf{0}_2 & \cdots & \mathbf{0}_2 & \mathbf{0}_2 & \mathbf{A}_M \end{array} \right], \quad (57)$$

$$\mathbf{B}_{cc} = \left[\begin{array}{c|ccccccc} \mathbf{J} & \mathbf{0}_2 & \mathbf{0}_2 & \mathbf{0}_2 & \cdots & \mathbf{0}_2 & \mathbf{0}_2 & \mathbf{0}_2 \\ \hline \mathbf{0}_2 & \mathbf{B}_0 & -\mathbf{I}_2 & \mathbf{0}_2 & \cdots & \mathbf{0}_2 & \mathbf{0}_2 & \mathbf{0}_2 \\ \mathbf{0}_2 & -\mathbf{I}_2 & \mathbf{B}_1 & \mathbf{I}_2 & \cdots & \mathbf{0}_2 & \mathbf{0}_2 & \mathbf{0}_2 \\ \mathbf{0}_2 & \mathbf{0}_2 & \mathbf{I}_2 & \mathbf{B}_2 & \cdots & \mathbf{0}_2 & \mathbf{0}_2 & \mathbf{0}_2 \\ \vdots & \vdots & \vdots & \vdots & \ddots & \vdots & \vdots & \vdots \\ \mathbf{0}_2 & \mathbf{0}_2 & \mathbf{0}_2 & \mathbf{0}_2 & \cdots & \mathbf{B}_{M-2} & \mp \mathbf{I}_2 & \mathbf{0}_2 \\ \mathbf{0}_2 & \mathbf{0}_2 & \mathbf{0}_2 & \mathbf{0}_2 & \cdots & \mp \mathbf{I}_2 & \mathbf{B}_{M-1} & \pm \mathbf{I}_2 \\ \mathbf{0}_2 & \mathbf{0}_2 & \mathbf{0}_2 & \mathbf{0}_2 & \cdots & \mathbf{0}_2 & \pm \mathbf{I}_2 & \mathbf{B}_M \end{array} \right], \quad (58)$$

$$\dot{\mathbf{z}} = \begin{bmatrix} \dot{v}_x \\ \dot{\omega}_y L \\ \dot{u} \\ \dot{\varphi} L \\ \dot{\mathbf{z}}_f \end{bmatrix}, \quad \mathbf{z} = \begin{bmatrix} v_x \\ \omega_y L \\ u \\ \varphi L \\ \mathbf{z}_f \end{bmatrix}, \quad \mathbf{f} = \begin{bmatrix} 0 \\ 0 \\ 0 \\ M_{sc}(t)/L \\ \mathbf{0} \end{bmatrix}, \quad (59)$$

where, according to [49], matrices \mathbf{C}_k (with $k = c, 1, \dots, M - 1$) in (32) change to 2×2 identity matrices, \mathbf{I}_2 ; similarly $\mathbf{A}_0 = \mathbf{T}_c$, $\mathbf{A}_1 = -\mathbf{T}_1$, \dots , $\mathbf{A}_M = \pm \mathbf{T}_M$ and $\mathbf{B}_0 = -\mathbf{S}_c$, $\mathbf{B}_1 = \mathbf{S}_1$, \dots , $\mathbf{B}_M = \mp \mathbf{S}_M$ are the 2×2 block-diagonal terms appearing in matrices \mathbf{A} and \mathbf{B} , see, for instance, (7)–(8) and (31)–(32).

It should be noticed that when in (57)–(58) there appear \pm or \mp , the upper sign holds when M is an even number, the lower one when M is odd.

Matrices \mathbf{A}_{cc} , (57), and \mathbf{B}_{cc} , (58) are banded with no more than $p = 3$ elements outside the main-diagonal; thus the so-called bandwidth b is given by $b = 2p + 1 = 7$; moreover, for $M = 7$ there are exactly $N = 2(M + 1) + 2 = 18$ state-variables including the internal DOFs.

The numerical stability of the system (56) is studied by means of the eigenvalues $\lambda_j = \alpha_j + i\beta_j$ ($j = 1, \dots, N$) of the eigenproblem $\lambda \mathbf{A}_{cc} \mathbf{x} = \mathbf{B}_{cc} \mathbf{x}$.

1 In order to allow potentially interested readers to reproduce the presented
 2 results, the ingredients for building system matrices \mathbf{A}_{cc} and \mathbf{B}_{cc} for the
 3 case of the elastic half-space soil are given in Appendix B. For the case of
 4 the stratum on bedrock and for other similar data, readers willing to make
 5 numerical experiments are invited to send a message to the authors.

6 For the half-space soil, Table 1 shows that there are three unstable mem-
 7 bers: one complex pair and one real eigenvalue with positive real part.

Table 1: Eigenvalues and corresponding vibration characteristics for the short-circuit problem, *horizontal and rocking motions*, half-space solution. An asterisk (*) marks eigenvalues to be modified by *deflation*.

j	α_j	β_j	$\ \lambda_j\ $
1, 2	-30.5377613398693	± 36.9665527530850	47.9487318924852
3, 4	-36.7984233637257	± 32.7541288282581	49.2641544873564
5, 6	-16.2610864194862	± 88.4164692503083	89.8993602103636
7, 8	-25.0359229832008	± 120.784488690714	123.351895599127
9, 10	-22.3272045634265	± 150.726477047897	152.371174921267
11	* 152.482140851938	0	152.482140851938
12, 13	* 8.10500398591369	± 175.763261659552	175.950036200098
14, 15	-57.3035477838088	± 201.858923868905	209.834986916204
16, 17	-6.42370613097185	± 397.101954620184	397.153907652472
18	-2751.30950243050	0	2751.30950243050

8 The corresponding dynamic response of the soil-foundation-rotor system
 9 due to the short-circuit torque is shown in Figure 6.

10 For the stratum on bedrock only one unstable real eigenvalue appears in
 11 Table 2.

Table 2: Eigenvalues and corresponding vibration characteristics for the short-circuit problem, *horizontal and rocking motions*, stratum on bedrock solution. An asterisk (*) marks eigenvalues to be modified by *deflation*.

j	α_j	β_j	$\ \lambda_j\ $
1, 2	-15.2645841513819	± 32.5810580205685	35.9796174389649
3, 4	-26.2850396191873	± 63.1075018576127	68.3627098533319
5, 6	-14.2097942649687	± 99.4842342949862	100.493935768843
7, 8	-8.14501162040569	± 104.820671438842	105.136646204766
9, 10	-8.61543766055009	± 134.759207778025	135.034328402239
11, 12	-11.9965504452661	± 152.037703945112	152.510264059463
13, 14	-20.9084707299802	± 164.304196721182	165.629203972184
15	-248.557968086746	0	248.557968086746
16	* 705.142315580316	0	705.142315580316
17, 18	-49.1789010052700	± 784.590309391712	786.130089676937

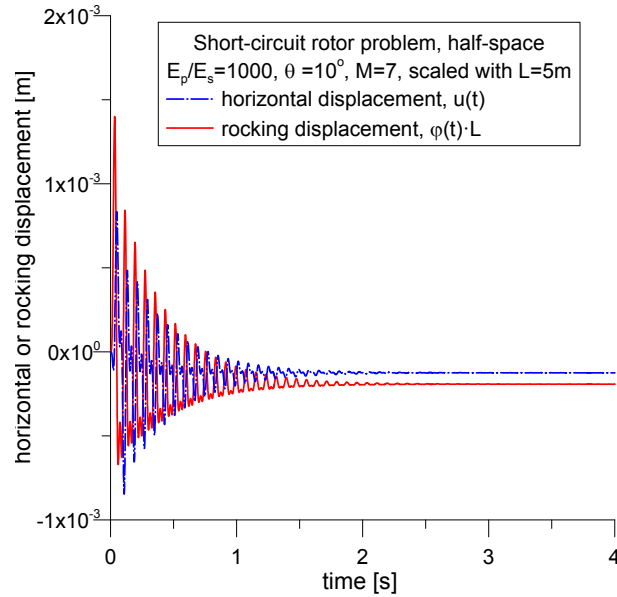


Figure 6: Dynamic response for the short-circuit problem, case of elastic half-space: time-history for both *horizontal* and *rocking* displacements.

The dynamic response of the soil-foundation-rotor system due to the short-circuit torque is shown for this case in Figure 7. 1
2

The integration of the system of first-order ODEs in (56) with the definitions (57)–(59) is performed by means of a linear interpolation given by (29), and recalled here for the reader’s convenience: 3
4
5

$$\mathbf{z} = \mathbf{z}_{k-1} \left(1 - \frac{\tau}{h}\right) + \mathbf{z}_k \frac{\tau}{h}$$

within a time-step h and solving the resulting system of linear algebraic 6

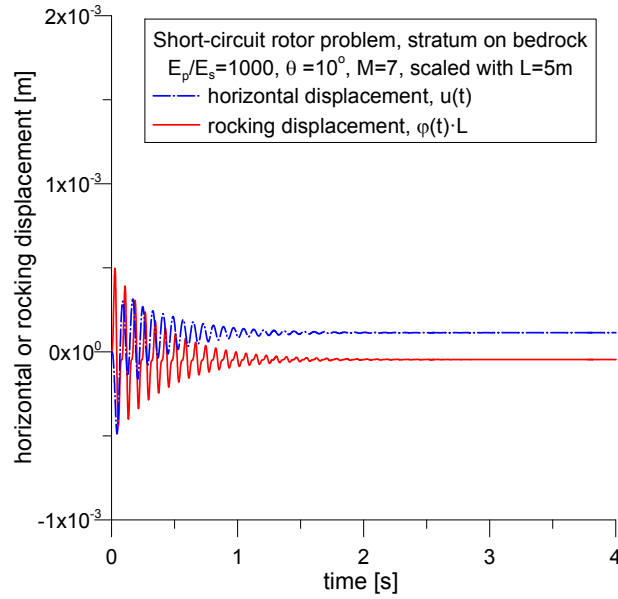


Figure 7: Dynamic response for the short-circuit problem, case of stratum on bedrock: time-history for both *horizontal* and *rocking* displacements.

1 equations:

$$(\mathbf{A}_{cc} - \frac{h}{2}\tilde{\mathbf{B}}_{cc})\mathbf{z}_k = (\mathbf{A}_{cc} + \frac{h}{2}\tilde{\mathbf{B}}_{cc})\mathbf{z}_{k-1} + \int_{k-1}^k \mathbf{f}(t)dt. \quad (60)$$

2 The deflated matrix $\tilde{\mathbf{B}}_{cc}$ contains its original \mathbf{B}_{cc} plus the parts from modal
3 deflation as shown in Section 2.

4 The operation counts (multiplications and divisions) for solving full and
5 banded $N \times N$ linear systems having a bandwidth $b = 2p + 1$ are approxi-

mately given as follows (see [8], [51]) in Table 3. 1

Table 3: Approximate operation counts for solving full and banded $N \times N$ systems of linear algebraic equations.

	Full matrix	Banded matrix
LU -decomposition	$N^3/3$	$Np(p+1)$
Back-substitution (for 1 r.h.s.)	N^2	$N(2p+1)$

Thus, in the present case, with $N = 18$ and $p = 3$ Table 4 shows the 2
benefits in terms of storage saving which can be achieved when the banded 3
properties of system matrices are exploited. 4

Table 4: Approximate operation counts when $N = 18$ and $p = 3$.

	Full matrix	Banded matrix
LU -decomposition	1944	216
Back-substitution (for 1 r.h.s.)	324	126

A total evaluation concerning the operation count has to include addi- 5
tional numerical aspects like those descending from time-step adaption due 6
to error-estimation as shown in [47]. Then, LU -decomposition of the coef- 7
ficient matrix has to be done several times. And even when the computer 8
operational speed is very high, the amount of operations should be minimized 9
in order to reduce numerical noise due to truncation errors and in order to 10
reduce time-delay in system control. 11

5. Conclusions 12

The consistent numerical description of radiation of energy towards infin- 13
ity for unbounded domains is still a challenge. A significant progress in this 14
matter has been provided by the Scaled Boundary Finite Element Method. 15
A typical outcome of this method is a set of impedances which is interpolated 16
in a rational manner using a least-squares approach. 17

The rational realization can be replaced by a linear state-space formula- 18
tion in the frequency-domain with significantly banded state-space matrices 19
 \mathbf{A} , \mathbf{B} using additional internal degrees of freedom. 20

1 Typically this process is numerically sensitive and can be contaminated by
 2 numerical noise and thus artificial unstable solutions. By means of spectral
 3 shifting in combination with deflation these spurious parts can be stabilized.
 4 However, deflation adds dyadic products to the state-space matrices and thus
 5 destroys their sparseness.

6 This paper presents an implicit procedure: the stabilized system with
 7 fully populated matrices due to deflation is nevertheless mainly treated by
 8 means of its banded non-deflated original state-space matrices \mathbf{A} , \mathbf{B} .

9 Thus the amount of arithmetic operations can be reduced significantly,
 10 compared with that resulting from treating the fully-populated, explicitly
 11 deflated, system matrices.

12 The procedure presented in this paper is useful in all those situations,
 13 where dyadic products are added to originally banded parents. Here, an
 14 application from transient soil-structure interaction with an unbounded soil-
 15 domain has been presented. Similar problems with coupled systems, includ-
 16 ing unbounded domains, are: soil-structure-soil interaction, dam-reservoir
 17 interaction, acoustic problems and diffusion, which is characterized by frac-
 18 tional derivatives.

19 In the field of system identification numerical noise is a problem, too, and
 20 can be treated by implicit deflation exactly as it has shown in this paper.

21 Acknowledgement

22 The financial support of MIUR, the Italian Ministry of Education, Uni-
 23 versity and Research, under grant PRIN 2010–2011 (project 2010MBJK5B—
 24 *Dynamic, Stability and Control of Flexible Structures*) is gratefully acknowl-
 25 edged.

26 Appendix A. Application of Sherman-Morrison method

27 A very simple example of the use of Sherman-Morrison method for solv-
 28 ing a 5×5 linear system of algebraic equations with a banded structure is
 29 illustrated. By making use of the same notation adopted in 3, let matrix
 30 $[\mathbf{A} - (h/2)\mathbf{B}]$, appearing in the l.h.s. of (41), have this expression:

$$\left[\mathbf{A} - \frac{h}{2} \mathbf{B} \right] = \begin{bmatrix} 4 & -2 & 0 & 0 & 0 \\ -2 & 3 & -1 & 0 & 0 \\ 0 & -1 & 3 & -1 & 0 \\ 0 & 0 & -1 & 2 & -1 \\ 0 & 0 & 0 & -1 & 2 \end{bmatrix}, \quad (\text{A.1})$$

whose tridiagonal banded structure is apparent. 1

Let moreover \mathbf{L} and $-(h/2)\mathbf{R}$, defined by (39)–(40), be: 2

$$\mathbf{L} = \begin{bmatrix} 2 & 6 \\ 0 & -5 \\ 1 & 1 \\ 0 & -1 \\ 1 & 2 \end{bmatrix}, \quad -\frac{h}{2} \mathbf{R} = \begin{bmatrix} 1 & 1 \\ 1 & -1 \\ 1 & 0 \\ 1 & 1 \\ 1 & -1 \end{bmatrix}. \quad (\text{A.2})$$

Thus, the correction due to deflation would be given in this case by: 3

$$-\frac{h}{2} \mathbf{L} \mathbf{R}^T = \begin{bmatrix} 8 & -4 & 2 & 8 & -4 \\ -5 & 5 & 0 & -5 & 5 \\ 2 & 0 & 1 & 2 & 0 \\ -1 & 1 & 0 & -1 & 1 \\ 3 & -1 & 1 & 3 & -1 \end{bmatrix}, \quad (\text{A.3})$$

which, when added to $[\mathbf{A} - \frac{h}{2} \mathbf{B}]$ would destroy its tri-diagonal structure, 4
resulting in a completely filled process matrix: 5

$$\left[\mathbf{A} - \frac{h}{2} \tilde{\mathbf{B}} \right] = \left[\mathbf{A} - \frac{h}{2} (\mathbf{B} - \mathbf{L} \mathbf{R}^T) \right] = \begin{bmatrix} 12 & -6 & 2 & 8 & -4 \\ -7 & 8 & -1 & -5 & 5 \\ 2 & -1 & 4 & 1 & 0 \\ -1 & 1 & -1 & 1 & 0 \\ 3 & -1 & 1 & 2 & 1 \end{bmatrix}. \quad (\text{A.4})$$

Let the r.h.s. of (41) be: 6

$$\mathbf{f}_k = [2 \quad -1 \quad 3 \quad -1 \quad 4]^T; \quad (\text{A.5})$$

then the *First step* of the procedure requires solving the linear system (41) 7
for the this r.h.s., resulting in the auxiliary variable \mathbf{w} : 8

$$\mathbf{w} = [1 \quad 1 \quad 2 \quad 2 \quad 3]^T. \quad (\text{A.6})$$

1 Now, considering that system (42) has to be solved twice— since in this
 2 case $n_d = 2$ —for these right-hand-sides, \mathbf{l}_1 and \mathbf{l}_2 , corresponding to the two
 3 columns of matrix \mathbf{L} :

$$\mathbf{l}_1 = [2 \ 0 \ 1 \ 0 \ 1]^T, \quad \mathbf{l}_2 = [6 \ -5 \ 1 \ -1 \ 2]^T, \quad (\text{A.7})$$

4 it is possible completing the *Second step* by loading the solutions into matrix
 5 \mathbf{X}^* , defined by (46):

$$\mathbf{X}^* = \begin{bmatrix} 1 & 1 \\ 1 & -1 \\ 1 & 0 \\ 1 & 0 \\ 1 & 1 \end{bmatrix}. \quad (\text{A.8})$$

6 Finally, before performing the *Third step* it is necessary to evaluate the two
 7 matrix products $\frac{h}{2}\mathbf{R}^T\mathbf{w}$ and $-\frac{h}{2}\mathbf{R}^T\mathbf{X}^*$, which give, respectively:

$$\frac{h}{2}\mathbf{R}^T\mathbf{w} = \begin{bmatrix} -9 \\ 1 \end{bmatrix}, \quad -\frac{h}{2}\mathbf{R}^T\mathbf{X}^* = \begin{bmatrix} 5 & 1 \\ 0 & 1 \end{bmatrix}. \quad (\text{A.9})$$

8 Then, solving (46), which assumes this simple form:

$$\begin{bmatrix} 6 & 1 \\ 0 & 2 \end{bmatrix} \mathbf{c} = \begin{bmatrix} -9 \\ 1 \end{bmatrix}, \quad (\text{A.10})$$

9 it is possible to compute the n_d components of column matrix \mathbf{c} :

$$\mathbf{c} = \frac{1}{12} \begin{bmatrix} -19 \\ 6 \end{bmatrix}. \quad (\text{A.11})$$

10 These are needed for completing the solution \mathbf{z}_k with a suitable combination
 11 of the solutions \mathbf{w} and $\mathbf{X}^*\mathbf{c}$:

$$\mathbf{z}_k = \begin{bmatrix} 1 \\ 1 \\ 2 \\ 2 \\ 3 \end{bmatrix} - \frac{19}{12} \begin{bmatrix} 1 \\ 1 \\ 1 \\ 1 \\ 1 \end{bmatrix} + \frac{1}{2} \begin{bmatrix} 1 \\ -1 \\ 0 \\ 0 \\ 1 \end{bmatrix} = \frac{1}{12} \begin{bmatrix} -1 \\ -13 \\ 5 \\ 5 \\ 23 \end{bmatrix}. \quad (\text{A.12})$$

12 In order to confirm the correctness of the above illustrated procedure,
 13 the same result may be obtained if system (33), with the completely filled

process matrix provided by the deflation procedure, see (A.4), is solved for
the original r.h.s. \mathbf{f}_k , namely (A.5):

$$\left[\mathbf{A} - \frac{h}{2} \tilde{\mathbf{B}} \right] \mathbf{z}_k = \mathbf{f}_k, \quad \Rightarrow \quad \mathbf{z}_k = \frac{1}{12} \begin{bmatrix} -1 & -13 & 5 & 5 & 23 \end{bmatrix}^T. \quad (\text{A.13})$$

Appendix B. System matrices for the short-circuit problem

The building blocks for assembling the complete system matrices \mathbf{A}_{cc}
and \mathbf{B}_{cc} , see (57)–(58), is the knowledge of the 2×2 matrices \mathbf{J} ; $\mathbf{A}_0, \dots, \mathbf{A}_M$;
 $\mathbf{B}_0, \dots, \mathbf{B}_M$.

Those which have been used in Section 4 in the case of a half-space
solution with $M = 7$ for analyzing the short-circuit problem, are given here
in a standard E20.15 Fortran format (with 15 significant figures, which are
suitable for the accuracy of double-precision variables):

$$\mathbf{J} = \begin{bmatrix} 0.2400000000000000E-4 & 0.672000001072884E-5 \\ 0.672000001072884E-5 & 0.1003840000000000E-4 \end{bmatrix}, \quad (\text{B.1})$$

$$\mathbf{A}_0 = \begin{bmatrix} 0.133644393751605E-2 & 0.287866237313723E-3 \\ -0.115858660105272E-1 & 0.184347527166318E-1 \end{bmatrix}, \quad (\text{B.2})$$

$$\mathbf{A}_1 = \begin{bmatrix} 0.843583416003512E-3 & -0.719778973913755E-3 \\ -0.115372067908800E-1 & -0.984058566993428E-3 \end{bmatrix}, \quad (\text{B.3})$$

$$\mathbf{A}_2 = \begin{bmatrix} 0.131228768389737E-2 & 0.153867486512852E-2 \\ 0.275038635221684E-1 & 0.133402120942196E-1 \end{bmatrix}, \quad (\text{B.4})$$

$$\mathbf{A}_3 = \begin{bmatrix} -0.864693318308295E-1 & 0.726481298490113E-2 \\ 0.279049021966555E-1 & 0.115813250447287E-2 \end{bmatrix}, \quad (\text{B.5})$$

$$\mathbf{A}_4 = \begin{bmatrix} 0.156528659882495E-3 & -0.535332491400231E-3 \\ -0.281535724524854E-2 & -0.614459018172883E-2 \end{bmatrix}, \quad (\text{B.6})$$

$$\mathbf{A}_5 = \begin{bmatrix} -0.717953332315951E+1 & 0.464138709812856E+0 \\ 0.192771932824898E+2 & -0.118200788200538E+1 \end{bmatrix}, \quad (\text{B.7})$$

$$\mathbf{A}_6 = \begin{bmatrix} -0.163876893880059E-3 & -0.656871935739603E-4 \\ -0.263837585498842E-2 & -0.102169192327277E-2 \end{bmatrix}, \quad (\text{B.8})$$

$$\mathbf{A}_7 = \begin{bmatrix} -0.218407123827608E+3 & 0.187549581862310E+2 \\ 0.829526018458060E+3 & -0.726433888669744E+2 \end{bmatrix}, \quad (\text{B.9})$$

$$\mathbf{B}_0 = \begin{bmatrix} -0.676435848824604E+0 & 0.343834535205479E+0 \\ -0.241177187997159E+1 & 0.170610729181941E+1 \end{bmatrix}, \quad (\text{B.10})$$

$$\mathbf{B}_1 = \begin{bmatrix} -0.129826388936489E+1 & 0.108289052669685E+0 \\ -0.525289313706782E+1 & 0.681327820621435E+0 \end{bmatrix}, \quad (\text{B.11})$$

$$\mathbf{B}_2 = \begin{bmatrix} 0.734396443982700E+0 & -0.179587118349401E+0 \\ 0.531296351564896E+1 & -0.862601076631469E+0 \end{bmatrix}, \quad (\text{B.12})$$

$$\mathbf{B}_3 = \begin{bmatrix} 0.115322613467869E+2 & -0.556511787230093E+0 \\ -0.495458854501284E+1 & 0.825211783729445E+0 \end{bmatrix}, \quad (\text{B.13})$$

$$\mathbf{B}_4 = \begin{bmatrix} 0.153580946855786E+0 & 0.666483376899730E-1 \\ 0.154173717831747E+1 & 0.110232361857816E+1 \end{bmatrix}, \quad (\text{B.14})$$

$$\mathbf{B}_5 = \begin{bmatrix} 0.814976785569525E+3 & -0.536895780820735E+2 \\ -0.153387036316747E+4 & 0.106600689152269E+3 \end{bmatrix}, \quad (\text{B.15})$$

$$\mathbf{B}_6 = \begin{bmatrix} 0.117508543431825E-1 & 0.606572280673132E-2 \\ 0.171184615236513E+0 & 0.933145449295855E-1 \end{bmatrix}, \quad (\text{B.16})$$

$$\mathbf{B}_7 = \begin{bmatrix} 0.189550702814661E+5 & -0.948935931008649E+3 \\ -0.858749448995366E+5 & 0.467857069789019E+4 \end{bmatrix}, \quad (\text{B.17})$$

1 With these ingredients, and taking into account that $\mathbf{0}_2$ and \mathbf{I}_2 in eqs. (57)–
 2 (58) denote respectively a square null matrix and an identity matrix of order
 3 2, the interested reader should be able to reproduce the same system
 4 matrices used for the first example.

5 To define the corrections produced by the deflation procedure it is neces-
 6 sary to know the eigenvalues λ_j which require shifting, and the corresponding
 7 right-, \mathbf{x}_j and left-eigenvectors, \mathbf{y}_j . Parameter ϵ used for shifting the eigen-
 8 values has always assumed to be equal to $2\alpha_j$, so that any shifted eigenvalue
 9 has been moved on the complex plane in a symmetric position, with reference
 10 to the imaginary axis, to its original one.

11 For the considered problem, looking at the complete list of eigenvalues
 12 ordered by increasing magnitude given by Table 1, it is clear that the three
 13 eigenvalues which require shifting are: λ_{11} (real) and λ_{12} – λ_{13} (a complex
 14 conjugate pair).

The corresponding eigenvectors, whose components are ordered according

to the same sequence appearing in Table 1, are the following:

$$\lambda_{11} = 152.482140851938;$$

$$\mathbf{x}_{11} = \begin{bmatrix} -0.100328487624792E+0 \\ 0.100000000000000E+1 \\ 0.655814506809039E-2 \\ 0.188868686452404E-2 \\ -0.824924754643652E-2 \\ 0.383567611215899E-2 \\ 0.200148560668322E-1 \\ -0.435223131105921E-2 \\ -0.619346206274143E-1 \\ 0.833535554543501E-2 \\ 0.201044637366518E-1 \\ -0.289997114316643E-3 \\ -0.450708732788741E-2 \\ 0.118769374039790E-2 \\ 0.156548495567518E-1 \\ 0.539663969809698E-5 \\ 0.737335359392647E-4 \end{bmatrix}, \quad \mathbf{y}_{11} = \begin{bmatrix} 0.100000000000000E+1 \\ 0.386739284516163E+0 \\ 0.655814506809041E-2 \\ 0.253629233138647E-2 \\ -0.114647127421046E-1 \\ -0.245185851984957E-2 \\ -0.183667967704952E-1 \\ 0.707451098252881E-2 \\ -0.133608238801449E-1 \\ -0.153372480830304E-1 \\ 0.170626831745806E+0 \\ -0.521345042616996E-2 \\ -0.150414623569745E-2 \\ -0.668817581517314E-3 \\ 0.513157142520315E-1 \\ -0.582350678586097E-3 \\ 0.471775083500828E-4 \\ 0.113678010114319E-4 \end{bmatrix}, \quad (\text{B.18})$$

$$\lambda_{12,13} = 8.10500398591369 \pm i 175.763261659552;$$

$$\mathbf{x}_{12,13} = \begin{bmatrix} 0.139537384952254E+0 \\ 0.130186352189687E+0 \\ -0.688073380315063E-4 \\ -0.286743714444453E-3 \\ -0.240374003571563E-2 \\ 0.875298036171494E-3 \\ -0.887543258800201E-3 \\ -0.996646484972821E-3 \\ -0.145844662052558E-1 \\ -0.435853038695098E-2 \\ 0.110826801219336E-1 \\ 0.488881307577057E-3 \\ 0.419776435942652E-2 \\ -0.415155431378067E-1 \\ 0.000000000000000E+0 \\ -0.706827421946735E-3 \\ -0.800352016096295E-2 \end{bmatrix} \pm i \begin{bmatrix} 0.109082600777154E+0 \\ -0.181228262129579E-1 \\ -0.743864415715844E-3 \\ -0.642382737898301E-3 \\ 0.177156933459235E-2 \\ -0.154261914357317E-2 \\ -0.428209489677169E-2 \\ -0.898318143640441E-3 \\ -0.407399925336061E-2 \\ 0.346392752002408E-2 \\ -0.134693739052809E-1 \\ -0.164171722346013E-3 \\ -0.436044168084241E-2 \\ -0.378171316722504E+0 \\ 0.100000000000000E+1 \\ 0.292019697260028E-3 \\ 0.515899190832424E-2 \end{bmatrix}, \quad (\text{B.19})$$

$$\mathbf{y}_{12,13} = \begin{bmatrix} 0.232406562398519E+0 \\ 0.597679555905942E-1 \\ 0.201258831718102E-3 \\ -0.181364517959250E-3 \\ 0.698014781161681E-3 \\ -0.145847219513284E-2 \\ -0.805365264947601E-2 \\ 0.637655565352687E-3 \\ -0.737626347763209E-3 \\ -0.295103891517964E-3 \\ -0.117519686449649E-1 \\ 0.139209068596705E-2 \\ 0.650962578483376E-3 \\ 0.851813854232112E-4 \\ 0.000000000000000E+0 \\ -0.244375447571072E-2 \\ -0.104979082949310E-2 \\ -0.248030042542863E-3 \end{bmatrix} \pm i \begin{bmatrix} -0.247321216457371E-1 \\ 0.347010946273614E-1 \\ 0.131298973736755E-2 \\ 0.348411352596378E-3 \\ -0.239467302422923E-3 \\ 0.791771194123920E-3 \\ 0.202450216138866E-2 \\ -0.333983674213373E-3 \\ 0.750739106579505E-3 \\ 0.442281841215438E-4 \\ -0.166933847983288E-1 \\ 0.109386971432206E-2 \\ -0.109262548700947E-2 \\ -0.278198167134854E-3 \\ 0.100000000000000E+1 \\ -0.647655525338316E-1 \\ 0.647877088375227E-3 \\ 0.178879269132340E-3 \end{bmatrix}. \quad (\text{B.20})$$

1

2 **References**

- 3 [1] C. Trinks, Consistent absorbing boundaries for time-domain interaction
4 analyses using the fractional calculus, Ph.D. thesis, Technische Univer-
5 sität Dresden, 2004.
- 6 [2] E. Zulkifli, Consistent description of radiation damping in transient
7 soil-structure interaction, Ph.D. thesis, Technische Universität Dresden,
8 2008.
- 9 [3] M. H. Bazyar, C. Song, A continued-fraction-based high-order transmit-
10 ting boundary for wave propagation in unbounded domains of arbitrary
11 geometry, *International Journal for Numerical Methods in Engineering*
12 74 (2008) 209–37.
- 13 [4] C. Birk, S. Prempramote, C. Song, An improved continued-fraction-
14 based high-order transmitting boundary for time-domain analyses in
15 unbounded domains, *International Journal for Numerical Methods in*
16 *Engineering* 89 (2012) 269–98.
- 17 [5] A. Cazzani, P. Ruge, Numerical aspects of coupling strongly frequency-
18 dependent soil-foundation models with structural finite elements in the
19 time-domain, *Soil Dynamics and Earthquake Engineering* 37 (2012)
20 56–72.

- [6] C. Birk, C. Song, A continued-fraction approach for transient diffusion in unbounded medium, *Computer Methods in Applied Mechanics and Engineering* 198 (2009) 2576–90.
- [7] J. Sherman, W. Morrison, Adjustment of an inverse matrix corresponding to a change in one element of a given matrix, *The Annals of Mathematical Statistics* 21 (1950) 124–7.
- [8] W. H. Press, S. A. Teukolsky, W. T. Vetterling, B. P. Flannery, *Numerical Recipes in Fortran — The art of scientific computing*, 2nd ed., Cambridge University Press, New York, 1992.
- [9] E. L. Yip, A note on the stability of solving a rank-p modification of a linear system by the Sherman-Morrison-Woodbury formula, *SIAM Journal on Scientific and Statistical Computing* 7 (1986) 507–13.
- [10] W. W. Hager, Updating the inverse of a matrix, *SIAM Review* 31 (1989) 221–39.
- [11] K. Riedel, A Sherman-Morrison-Woodbury identity for rank augmenting matrices with application to centering, *SIAM Journal on Matrix Analysis and Applications* 13 (1992) 659–62.
- [12] R. Bru, J. Cerdán, J. Marín, J. Mas, Preconditioning sparse nonsymmetric linear systems with the Sherman-Morrison formula, *SIAM Journal on Scientific Computing* 25 (2003) 701–15.
- [13] N. Egidi, P. Maponi, A Sherman-Morrison approach to the solution of linear systems, *Journal of Computational and Applied Mathematics* 189 (2006) 703–18.
- [14] P. Maponi, The solution of linear systems by using the Sherman-Morrison formula, *Linear Algebra and its Applications* 420 (2007) 276–94.
- [15] M. Batista, A. Karawia, The use of the Sherman-Morrison-Woodbury formula to solve cyclic block tri-diagonal and cyclic block penta-diagonal linear systems of equations, *Applied Mathematics and Computation* 210 (2009) 558–63.

- 1 [16] J. Yin, Preconditioner based on the Sherman-Morrison formula for regu-
2 larized least squares problems, *Applied Mathematics and Computation*
3 215 (2009) 3007–16.
- 4 [17] C. Deng, A generalization of the Sherman-Morrison-Woodbury formula,
5 *Applied Mathematics Letters* 24 (2011) 1561–4.
- 6 [18] A. Malyshev, M. Sadkane, Using the Sherman-Morrison-Woodbury in-
7 version formula for a fast solution of tridiagonal block Toeplitz systems,
8 *Linear Algebra and its Applications* 435 (2011) 2693–707.
- 9 [19] H. Saberi Najafi, S. Edalatpanah, G. Gravvanis, An efficient method
10 for computing the inverse of arrowhead matrices, *Applied Mathematics*
11 *Letters* 33 (2014) 1–5.
- 12 [20] E. D. Nino Ruiz, A. Sandu, J. Anderson, An efficient implementation
13 of the ensemble Kalman filter based on an iterative Sherman-Morrison
14 formula, *Statistics and Computing* 25 (2015) 561–77.
- 15 [21] M. Akgün, J. Garcelon, R. Haftka, Fast exact linear and non-linear
16 structural reanalysis and the Sherman-Morrison-Woodbury formulas,
17 *International Journal for Numerical Methods in Engineering* 50 (2001)
18 1587–606.
- 19 [22] M. Özer, T. Royston, Application of Sherman-Morrison matrix inver-
20 sion formula to damped vibration absorbers attached to multi-degree of
21 freedom systems, *Journal of Sound and Vibration* 283 (2005) 1235–49.
- 22 [23] M. B. Özer, H. Özgüven, T. Royston, Identification of structural non-
23 linearities using describing functions and the Sherman-Morrison method,
24 *Mechanical Systems and Signal Processing* 23 (2009) 30–44.
- 25 [24] O. Cakar, K. Sanliturk, Elimination of transducer mass loading effects
26 from frequency response functions, *Mechanical Systems and Signal Pro-*
27 *cessing* 19 (2005) 87–104.
- 28 [25] J. E. Mottershead, Y. M. Ram, Inverse eigenvalue problems in vibra-
29 tion absorption: Passive modification and active control, *Mechanical*
30 *Systems and Signal Processing* 20 (2006) 5–44.

- [26] D. Stăncioiu, H. Ouyang, Approximate inversion formula for structural dynamics and control, *Mechanical Systems and Signal Processing* 40 (2013) 344–55. 1
2
3
- [27] F. D’Annibale, A. Luongo, A damage constitutive model for sliding friction coupled to wear, *Continuum Mechanics and Thermodynamics* 25 (2013) 503–22. 4
5
6
- [28] N. Roveri, A. Carcaterra, Unsupervised identification of damage and load characteristics in time-varying systems, *Continuum Mechanics and Thermodynamics* 27 (2015) 531–50. 7
8
9
- [29] A. Carcaterra, N. Roveri, Tire grip identification based on strain information: Theory and simulations, *Mechanical Systems and Signal Processing* 41 (2013) 564–80. 10
11
12
- [30] H. Altenbach, V. Eremeyev, Eigen-vibrations of plates made of functionally graded material, *Computers, Materials and Continua* 9 (2009) 153–77. 13
14
15
- [31] H. Altenbach, V. Eremeyev, L. Lebedev, On the spectrum and stiffness of an elastic body with surface stresses, *ZAMM Zeitschrift für Angewandte Mathematik und Mechanik* 91 (2011) 699–710. 16
17
18
- [32] A. Luongo, D. Zulli, G. Piccardo, A linear curved-beam model for the analysis of galloping in suspended cables, *Journal of Mechanics of Materials and Structures* 2 (2007) 675–94. 19
20
21
- [33] G. Piccardo, F. Tubino, Dynamic response of Euler-Bernoulli beams to resonant harmonic moving loads, *Structural Engineering and Mechanics* 44 (2012) 681–704. 22
23
24
- [34] N. Roveri, A. Carcaterra, Damage detection in structures under traveling loads by Hilbert-Huang transform, *Mechanical Systems and Signal Processing* 28 (2012) 128–44. 25
26
27
- [35] M. Ferretti, G. Piccardo, Dynamic modeling of taut strings carrying a traveling mass, *Continuum Mechanics and Thermodynamics* 25 (2013) 469–88. 28
29
30

- 1 [36] F. dell’Isola, A. Madeo, L. Placidi, Linear plane wave propagation and
2 normal transmission and reflection at discontinuity surfaces in second
3 gradient 3d continua, *ZAMM Zeitschrift für Angewandte Mathematik
4 und Mechanik* 92 (2011) 52–71.
- 5 [37] F. dell’Isola, P. Seppecher, A. Madeo, How contact interactions may
6 depend on the shape of Cauchy cuts in N th gradient continua: approach
7 à la D’Alembert, *Zeitschrift für Angewandte Mathematik und Physik
8 (ZAMP)* 63 (2012) 1119–41.
- 9 [38] A. Madeo, I. Djeran-Maigre, G. Rosi, C. Silvani, The effect of fluid
10 streams in porous media on acoustic compression wave propagation,
11 transmission, and reflection, *Continuum Mechanics and Thermodynam-
12 ics* 25 (2013) 173–96.
- 13 [39] G. Rosi, I. Giorgio, V. Eremeyev, Propagation of linear compression
14 waves through plane interfacial layers and mass adsorption in second
15 gradient fluids, *ZAMM Zeitschrift für Angewandte Mathematik und
16 Mechanik* 93 (2013) 914–27.
- 17 [40] A. Madeo, T. Lekszycki, F. dell’Isola, A continuum model for the bio-
18 mechanical interactions between living tissue and bio-resorbable graft
19 after bone reconstructive surgery, *Comptes Rendus - Mecanique* 339
20 (2011) 625–40.
- 21 [41] A. Madeo, D. George, Y. Rémond, Second-gradient models accounting
22 for some effects of microstructure on remodelling of bones reconstructed
23 with bioresorbable materials, *Computer Methods in Biomechanics and
24 Biomedical Engineering* 16 (2013) 260–1.
- 25 [42] U. Andreaus, I. Giorgio, A. Madeo, Modeling of the interaction between
26 bone tissue and resorbable biomaterial as linear elastic materials with
27 voids, *Zeitschrift für Angewandte Mathematik und Physik (ZAMP)* 66
28 (2015) 209–37.
- 29 [43] A. C. Antoulas, *Approximation of large-scale dynamical systems*, SIAM,
30 Philadelphia, PA, 2005.
- 31 [44] X. Du, M. Zhao, Stability and identification for rational approximation
32 of frequency response function of unbounded soil, *Earthquake Engineer-
33 ing & Structural Dynamics* 39 (2010) 165–86.

- [45] J. H. Wilkinson, C. Reinsch, Handbook for Automatic Computation, 1
Vol. II, Linear Algebra, Springer-Verlag, New York, 1971. 2
- [46] E. Anderson, Z. Bai, C. Bischof, S. Blackford, J. Demmel, J. Dongarra, 3
J. D. Croz, A. Greenbaum, S. Hammarling, A. McKenney, D. Sorensen, 4
LAPACK Users' Guide, 3rd ed., SIAM, Philadelphia, 1999. 5
- [47] P. Ruge, A priori local error estimation with adaptive time-stepping, 6
Communications in Numerical Methods in Engineering 15 (1999) 479– 7
91. 8
- [48] DIN 4024 part 2., Maschinenfundamente (Machine foundations), Beuth- 9
Verlag, Berlin, 1988. 10
- [49] A. Cazzani, P. Ruge, Rotor platforms on pile-groups running through 11
resonance: a comparison between unbounded soil and soil-layers resting 12
on a rigid bedrock, Soil Dynamics and Earthquake Engineering 50 (2013) 13
151–61. 14
- [50] L. A. Padrón, J. J. Aznárez, O. Maeso, M. Saitoh, Impedance functions 15
of end-bearing inclined piles, Soil Dynamics and Earthquake Engineering 16
38 (2012) 97–108. 17
- [51] A. George, J. Liu, Computer Solution of Large Sparse Positive Definite 18
Systems, Prentice-Hall, Inc., Englewood Cliffs, NJ, 1981. 19